Supplemental Material

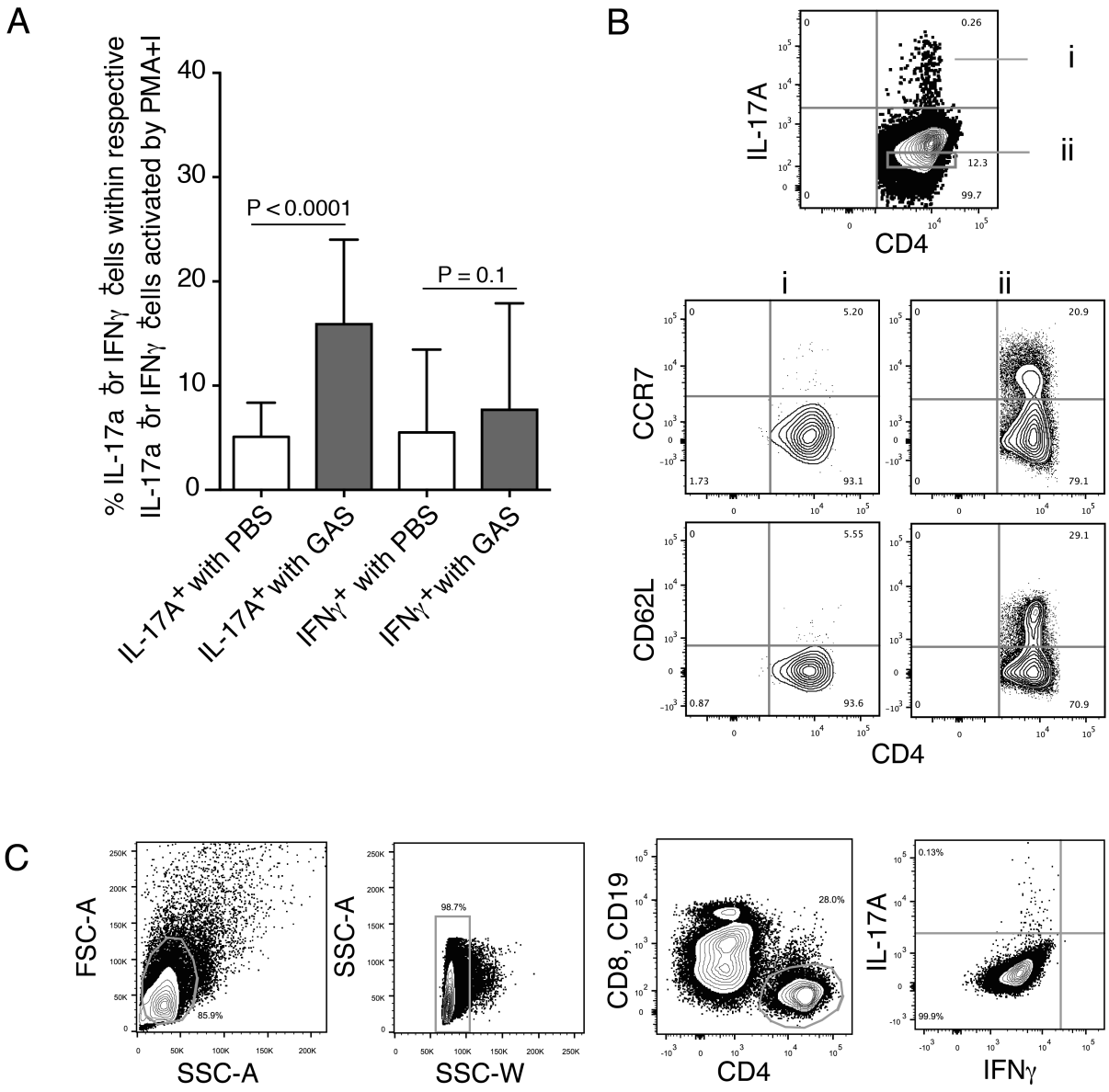

Supplemental Figure 1. GAS activation of IL-17A$^+$ or IFNγ$^+$ CD4$^+$ T cells expressed as a percentage of total cells that produce these signature cytokines with PMA+I activation. (A) Bar graph shows the percentage of T cells activated by PBS (control) or by HK-GAS. Single cell suspensions of tonsil tissue from 28 patients were incubated for 6 h with PBS (control), HK-GAS or

PMA+I prior to FACs analysis. Percentages shown on the Y axis were calculated from percentages of IL-17A$^+$ or IFNγ$^+$ CD4$^+$ cells that were activated by PBS or HK-GAS divided by percentages of IL-17A$^+$ or IFNγ$^+$ CD4$^+$ T cells, respectively, that were separately incubated with PMA+I as described in the methods. Bar graph shows mean ± s.e.m. Statistical significance of mean differences was assessed by the Wilcoxon matched-pairs signed rank test; vertical lines indicated the upper 95% confidence interval. Data were collected from >10 experiments. (B) FACS plots for HK-GAS-activated tonsil cells stained for IL-17A, CD4, CCR7 and CD62L. Cells in Panel i were gated on IL-17A$^+$ CD4$^+$ T cells and those in panel ii were gated on IL-17A$^-$ CD4$^+$ T cells. (C) FACS plots showing the gating strategy used in Figure1 and Supplemental Figure 1.

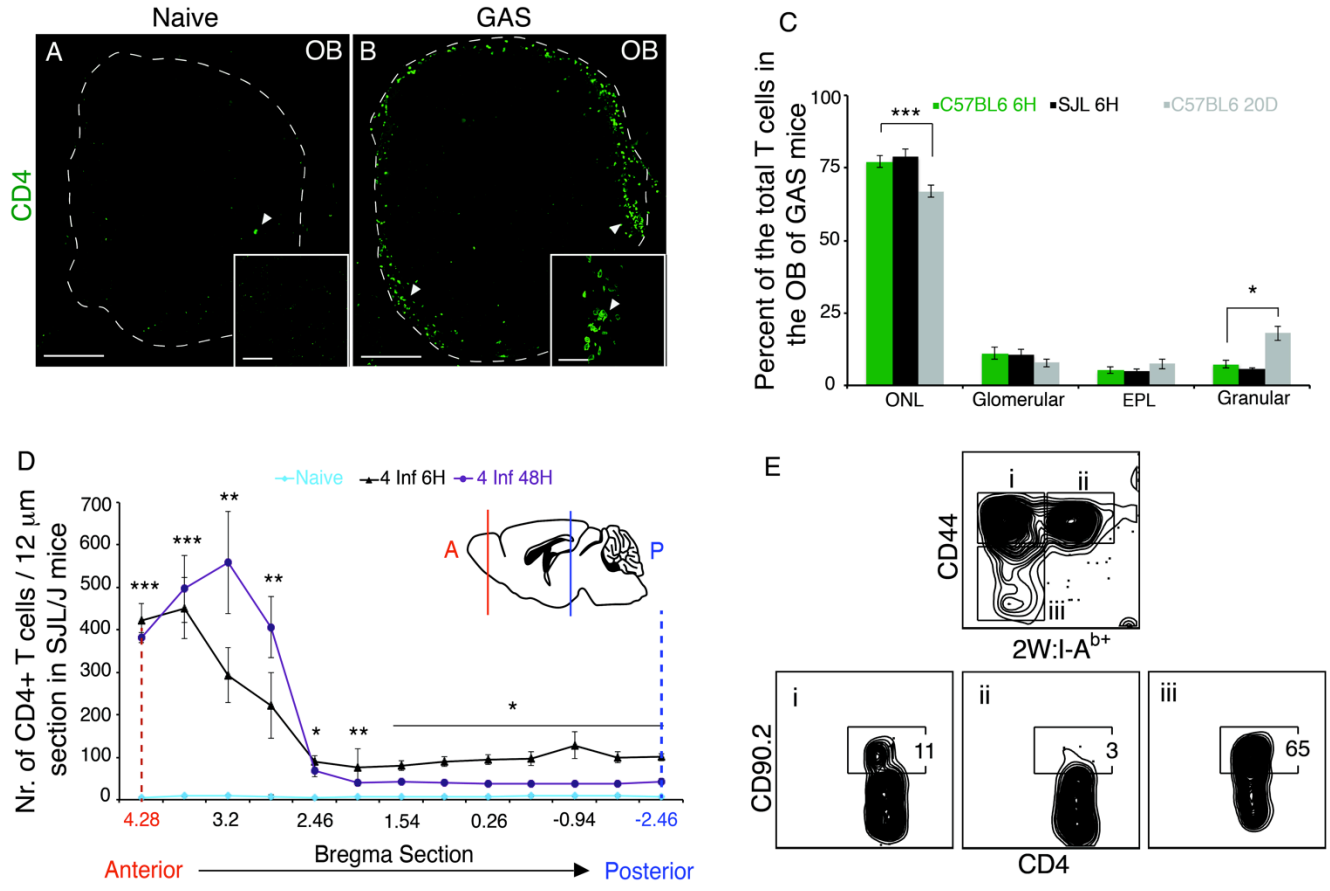

Supplemental Figure 2. T cells initially populate the olfactory bulb and associate with the olfactory sensory axons. (A, B) Lower magnification and inset (white box) of $CD4^+$ T cell (green) distribution in the OB from naive or multiply GAS-inoculated animals. Scale bars in lower magnifications are 250 µm, whereas in the insets 15 µm. (C) Bar graph of T cell distribution (Y axis) in various OB layers at 6h in multiply GAS-inoculated C57BL/6 (green bars) and SJL/J mice (black bars) and also 20 days (grey bar) after the last inoculation. Data were collected from n = 3-4 animals/group and presented as mean ± s.e.m. (C) Line graph of $CD4^+$ T cell distribution along the anterioposterior axis of the brain in multiply inoculated-SJL/J mice at 6 h (black) and 48 h (purple) after the final inoculation, or in naive (aqua) animals. Data were collected from multiple sections from n = 3-4 animals per group and presented as mean ± s.e.m. Statistical significance of *p<0.05, **p<0.001, ***p<0.0001; was assessed by either one-way ANOVA with Tukey's multiple post hoc comparison (C) or two way

ANOVA with Bonferroni post-hoc correction (D). (E) Representative FACS plot from GAS-inoculated mice showing the percentage of residual intravascular brain $CD4^+$ T cells that stain with anti-CD90.2 antibody injected i.v. a few minutes before sacrifice (see Materials and Methods for details). Lower panels are brain-derived $CD4^+$ T cells gated on: i) $CD44^{hi}$ 2W:I-A^{b-} ii) $CD44^{hi}$ 2W:I-A^{b+} and iii) $CD44^{low}$.

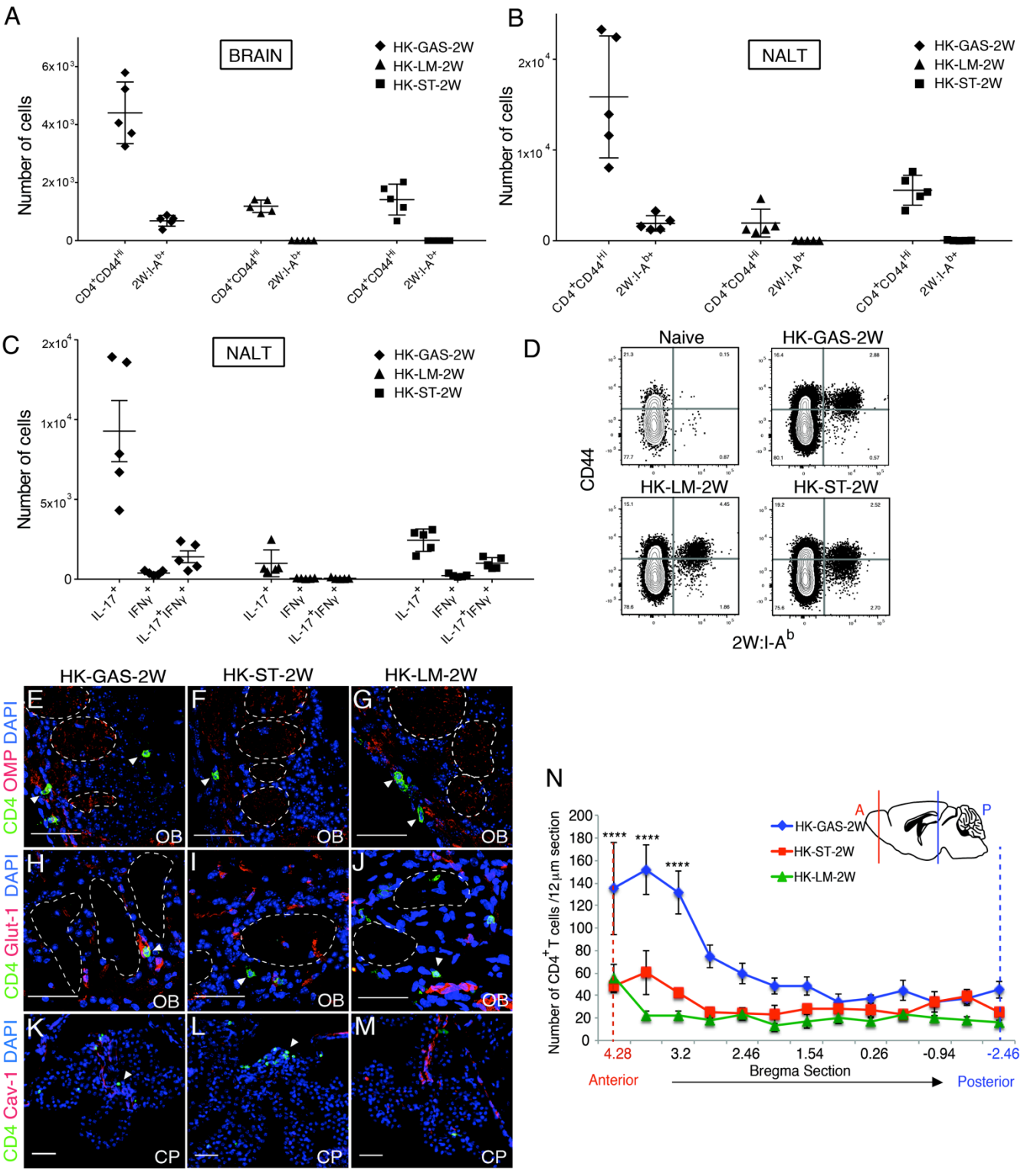

Supplemental Figure 3. Contrary to GAS, multiple i.n. inoculations with *Listeria monocytogenes* or *Salmonella typhimurium* do not cause significant T cell migration into the brain. (A) Scatter plot showing total numbers of either $CD4^{+}CD44^{Hi}$ cells or $2W{:}I\text{-}A^{b+}$ T cells isolated from brains of mice

inoculated i.n. with $2x10^8$ CFU of heat-killed *Streptococcus pyogenes* (HK-GAS-2W), *Salmonella typhimurium* (HK-ST-2W), or *Listeria monocytogenes* (HK-LM-2W) and analyzed by FACS. Scatter plots showing total numbers of either $CD4^+CD44^{hi}$ cells or 2W:I-A^{b+} T cells (B) or IL-17^+, IFNγ^+ or IL-17^+IFNγ^+ double positive $CD4^+$ T cells (C) in the NALT of the above mice. The lines in the plots represent mean ± s.e.m. (D) FACS plot showing 2W:I-$A^{b+}CD4^+$ T cells (indicated by red arrows) isolated from spleens of mice that were naïve or i.v. inoculated with $2x10^8$ CFU of HK-GAS-2W, HK-LM-2W or HK-ST-2W (seven days after a single inoculation). A representative plot is shown per group (n=2 per group). (E – M) Detection of $CD4^+$ T cells in brains of mice inoculated i.n. with HK-GAS-2W, HK-LM-2W or HK-ST-2W and analyzed by immunofluorescence from an independent experiment. $CD4^+$ T cells associate with olfactory marker protein (OMP, E-G), Glut-1^+ blood vessels (H-J), and the choroid plexus (CP, K-M). Scale bars = 50 μm. (N) Line graph of $CD4^+$ T cell distribution along the anteroposterior axis after multiple inoculations with HK-GAS-2W (blue, n=5 mice), HK-ST-2W (red, n=4 mice), or HK-LM-2W (green, n=4 mice). The X axis represents bregma sections, and Y axis the number of $CD4^+$ T cells per 12 μm section. Red and blue lines (solid) indicate positions of brain regions relative to the graph (dashed lines). Data are presented as mean ± s.e.m; ****$p<0.0001$ for HK-GAS-2W vs. HK-LM-2W and for HK-GAS-2W vs. HK-ST-2W by two-way ANOVA with Bonferroni post-hoc correction.

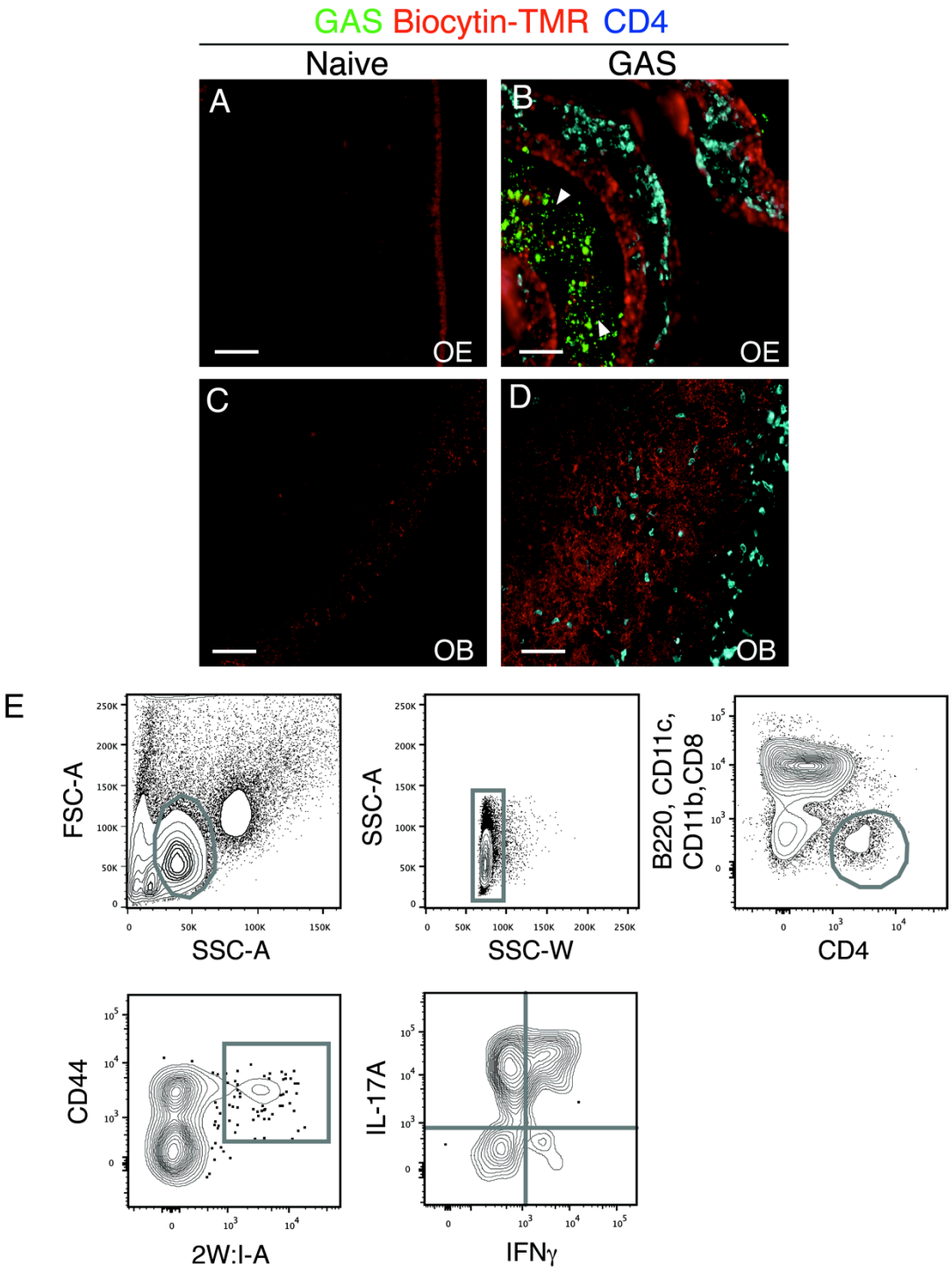

Supplemental Figure 4. T cell migration into the brain does not require tissue infection. (A-D) Immunofluorescence detection of streptococci (green), $CD4^+$ T cells (blue) and biocytin-TMR (red) in olfactory epithelia (OE, A, B) and olfactory bulb (OB, C,D) in 12 μm sections from naive and GAS i.n.

inoculated mice. Streptococci (green, white arrowheads) are labeled with a group A carbohydrate antibody. Visualization of $CD4^+$ labels T cells (blue) and biocytin-TMR (red) indicates BBB leakage in the OB (lower right panel). Scale bars (B) = 50 μm. (C) FACS plots showing the gating strategy used in Figures 2A, 2B and 3.

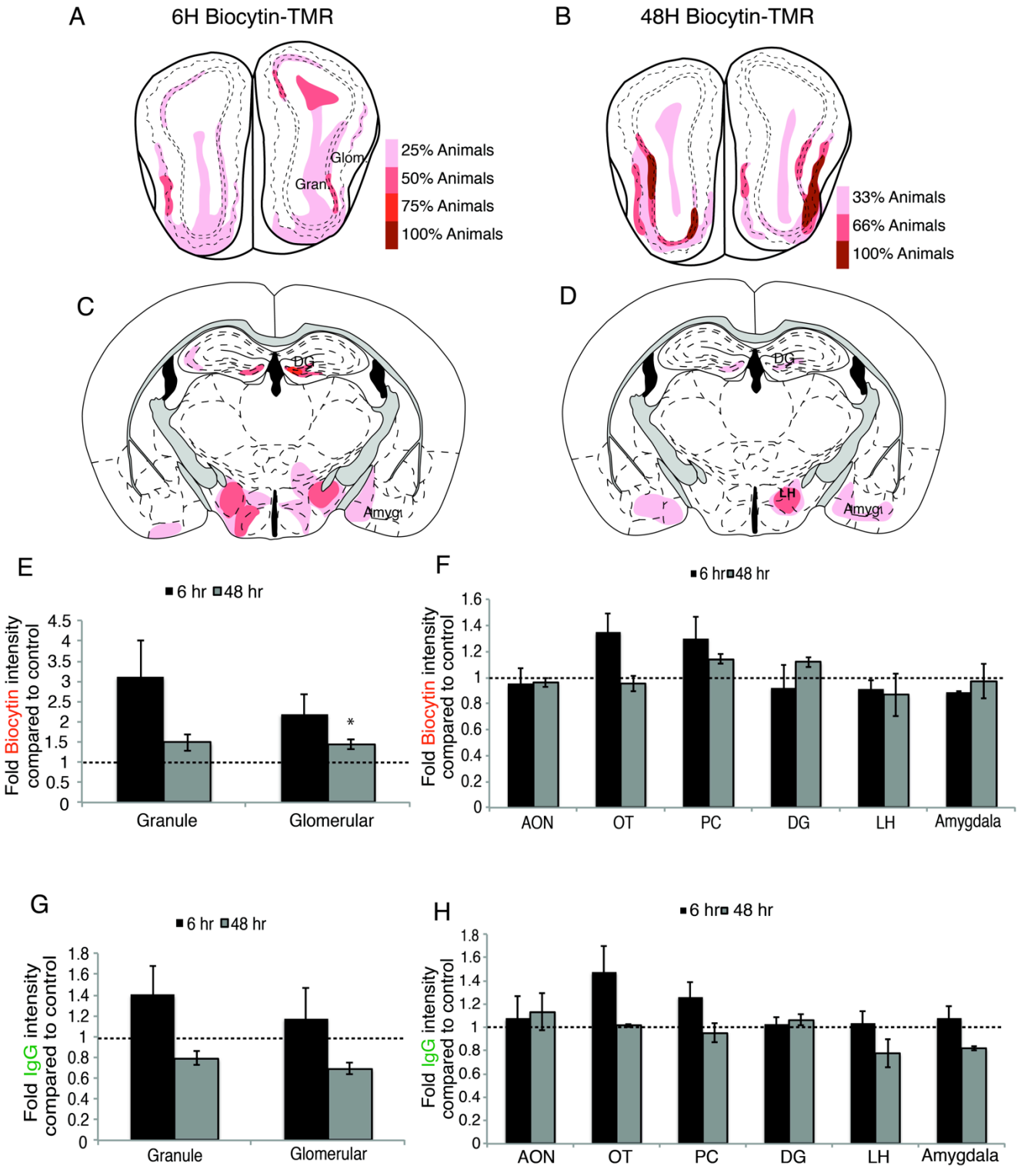

Supplemental Figure 5. Minimal BBB leakage, but no serum IgG deposition is found in brains of mice following a single GAS infection. (A-D) Heat maps of biocytin-TMR leakage in the OB (A, B) and posterior brain (C, D) in C57BL6/J mice after 6 or 48 h after one GAS inoculation, respectively.

Red hues represent percentages of animals showing biocytin-TMR leakage in various brain regions, not the intensity of tracer leakage observed among animals (see legend in A). (E-F) Bar graphs compare the fold change in biocytin-TMR average intensity between singly GAS-inoculated and naive mice in either the OB or other CNS regions [anterior olfactory nucleus (AON), olfactory tubercle (OT), piriform cortex (PC) and dentate gyrus (DG), lateral hypothalamus (LH) and amygdala] at 6 h (black bars) and 48 h (grey bars) after the inoculation. Data were collected from n = 3-4 animals in two independent experiments and presented as mean ± s.e.m, *$p<0.05$; two-tailed Student's t-test. (G-H) Bar graphs compare the fold change in IgG average intensities between singly GAS-inoculated and naive mice in either the OB, or other CNS regions (H) at 6 h (black bars) and 48 h (grey bars) after the inoculation. Data were collected from two independent experiments in n = 3-4 animals and presented as mean ± s.e.m, *$p<0.05$; two-tailed Student's t-test.

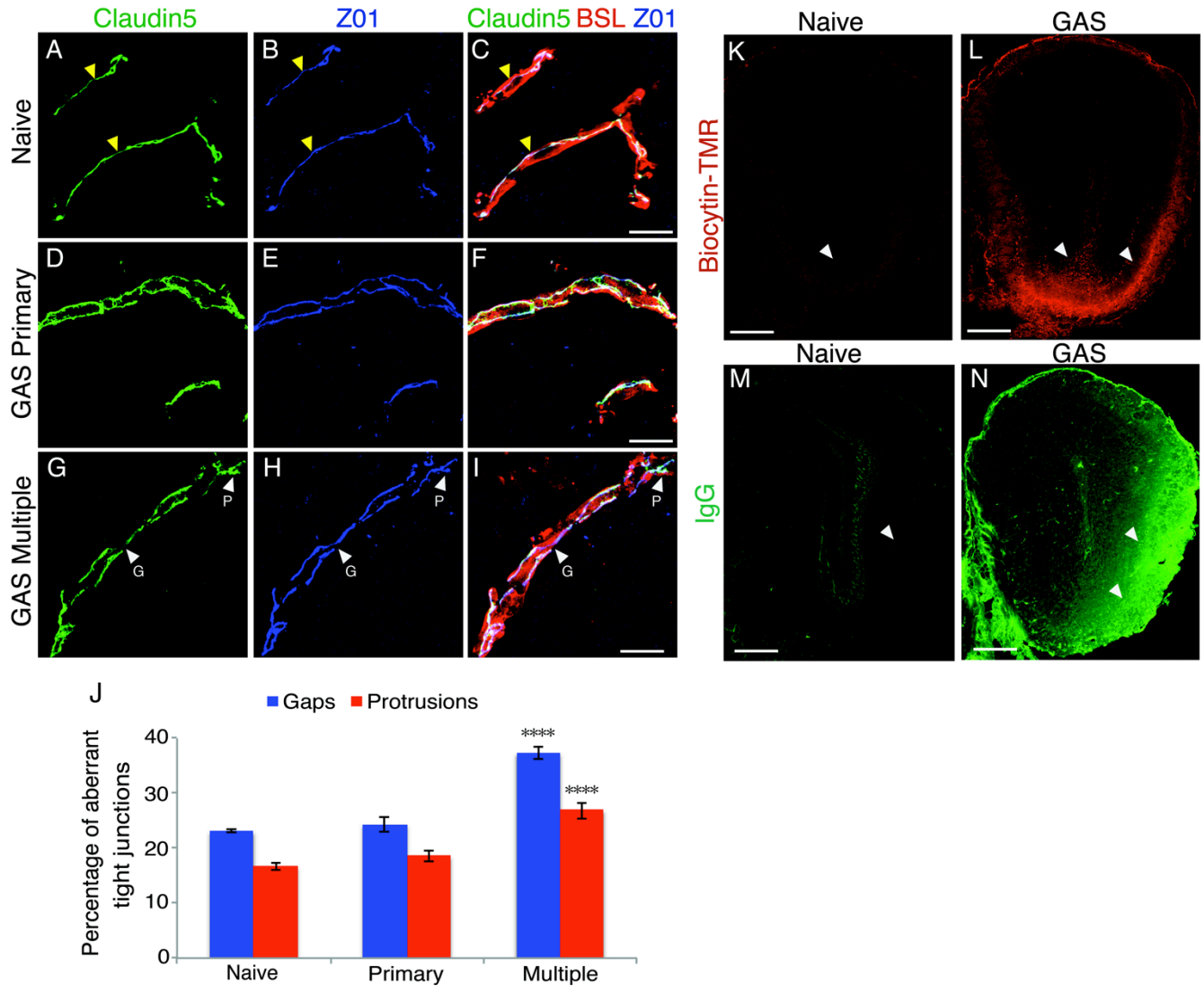

Supplemental Figure 6. Brain homing of T cells induces endothelial cell tight junction abnormalities. (**A-I**) Representative images of endothelial cell tight junctions (TJs) in the glomerular layer of the OB from naive, primary or multiply GAS-inoculated mice. TJs are labeled for Claudin-5 (A, D, G, green) and ZO1 (B, E, H, blue) and blood vessels labeled with BSL-rhodamine (C, F, I; red) in merged panels with Claudin-5 and ZO1. Yellow arrowheads point to normal junctions. TJ strands have many gaps (G, white arrowhead) or protrusions (P, white arrowhead) in mice with multiple GAS inoculations (panels G-I). (J) Bar graph comparing the fraction of aberrant TJs with gaps (blue bars) or protrusions (red bars) in naive, primary or multiple GAS inoculations. Panels K-N show low-magnification images of the OB sections with biocytin-TMR leakage and IgG deposition. Data were

collected from 10 independent sections per animal from n = 3 animals/group and presented as mean ± s.e.m, ****p<0.001, one-way ANOVA with Tukey's multiple post hoc comparison. Scale bars (A-I) = 15 μm and (K-N) = 250 μm.

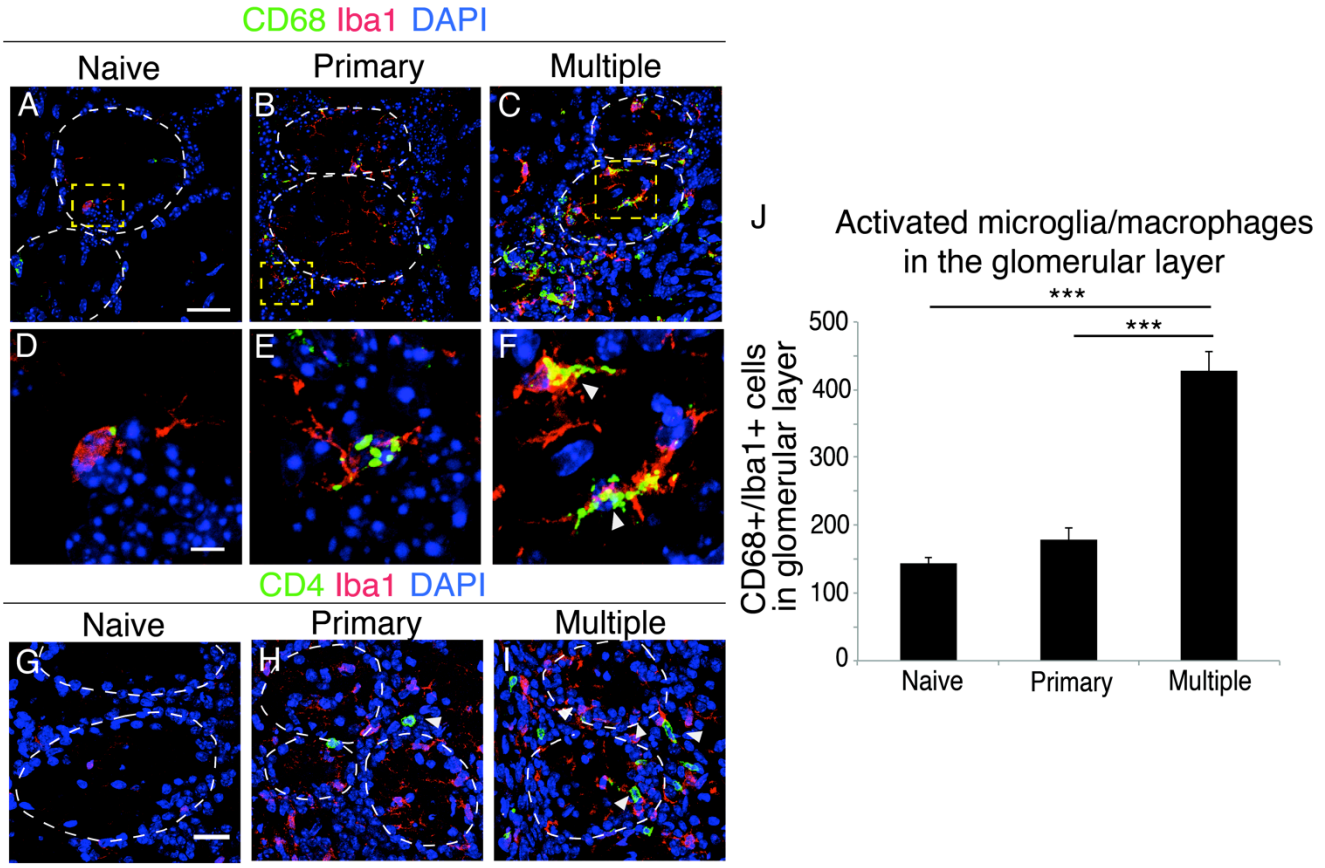

1180

1181 **Supplemental Figure 7. T cell homing into the brain is associated with microglia activation.** (A-F)
1182 Representative images of activated microglia ($CD68^+$ $Iba1^+$ double positive cells; yellow) in the OBs
1183 from naive, singly or multiply GAS-inoculated mice. Glomeruli are outlined with dashed white lines.
1184 The yellow dashed boxes show the region in images D-F. (G-I) Microglia ($Iba1^+$; red) are in close
1185 proximity to $CD4^+$ T cells (green). (G) Bar graph showing the number of activated microglia ($CD68^+$
1186 $Iba1^+$) in 12 μm sections of glomeruli from naive, singly or multiply GAS-inoculated mice. Data were
1187 collected from multiple sections of n = 3-4 animals per group (stained 3 independent times) and
1188 presented as mean ± s.e.m. **p<0.001, ***p<0.0001, one-way ANOVA with Tukey's multiple post hoc
1189 comparison. Scale bars (A-C; G-I) = 50 μm and (D-F) = 10 μm.